



# HHS Public Access

Author manuscript

*Nanotoxicology*. Author manuscript; available in PMC 2016 October 31.

Published in final edited form as:

*Nanotoxicology*. 2011 December ; 5(4): 568–582. doi:10.3109/17435390.2010.537791.

## The role of hypoxia inducible factor-1 $\alpha$ in the increased MMP-2 and MMP-9 production by human monocytes exposed to nickel nanoparticles

RONG WAN<sup>1,\*</sup>, YIQUN MO<sup>1,\*</sup>, SUFAN CHIEN<sup>2</sup>, YIHUA LI<sup>1</sup>, YIXIN LI<sup>1</sup>, DAVID J. TOLLERUD<sup>1</sup>, and QUNWEI ZHANG<sup>1</sup>

<sup>1</sup>Department of Environmental and Occupational Health Sciences, School of Public Health and Information Sciences

<sup>2</sup>Department of Surgery, University of Louisville, Louisville, Kentucky, USA

### Abstract

Nickel is an important economic commodity, but it can cause skin sensitization and may cause lung diseases such as lung fibrosis, pneumonitis, bronchial asthma and lung cancer. With development of nanotechnology, nano-sized nickel (Nano-Ni) and nano-sized titanium dioxide (Nano-TiO<sub>2</sub>) particles have been developed and produced for many years with new formulations and surface properties to meet novel demands. Our previous studies have shown that Nano-Ni instilled into rat lungs caused a greater inflammatory response as compared with standard-sized nickel (5  $\mu$ m) at equivalent mass concentrations. Nano-Ni caused a persistent high level of inflammation in lungs even at low doses. Recently, several studies have shown that nanoparticles can translocate from the lungs to the circulatory system. To evaluate the potential systemic effects of metal nanoparticles, we compared the effects of Nano-Ni and Nano-TiO<sub>2</sub> on matrix metalloproteinases 2 and 9 (MMP-2 and MMP-9) gene expression and activity. Our results showed that exposure of human monocyte U937 to Nano-Ni caused dose- and time- dependent increase in MMP-2 and MMP-9 mRNA expression and pro-MMP-2 and pro-MMP-9 activity, but Nano-TiO<sub>2</sub> did not. Nano-Ni also caused dose- and time- related increase in tissue inhibitor of metalloproteinases 1 (TIMP-1), but Nano-TiO<sub>2</sub> did not. To determine the potential mechanisms involved, we measured the expression of hypoxia inducible factor 1 $\alpha$  (HIF-1 $\alpha$ ) in U937 cells exposed to Nano-Ni and Nano-TiO<sub>2</sub>. Our results showed that exposure to Nano-Ni caused HIF-1 $\alpha$  accumulation in the nucleus. Furthermore, pre-treatment of U937 cells with heat shock protein 90 (Hsp90) inhibitor, 17-(Allylamino)-17-demethoxygeldanamycin (17-AAG), prior to exposure to Nano-Ni significantly abolished Nano-Ni-induced MMP-2 and MMP-9 mRNA upregulation and

Correspondence: Dr. Qunwei Zhang, MD, MPH, PhD, Department of Environmental and Occupational Health Sciences, School of Public Health and Information Sciences, University of Louisville, 485 E. Gray Street, Louisville, KY 40209, USA. Tel: +1 (502) 852 7200. Fax: +1 (502) 852 7246. Qunwei.Zhang@louisville.edu.

\*Rong Wan and Yiqun Mo contributed equally to this work.

The results was presented in part at 2009 ATS International Conference in San Diego, May 15–20, 2009.

#### Declaration of interest:

The authors report no conflict of interest. The authors alone are responsible for the content and writing of the paper.

Copyright of *Nanotoxicology* is the property of Taylor & Francis Ltd and its content may not be copied or emailed to multiple sites or posted to a listserv without the copyright holder's express written permission. However, users may print, download, or email articles for individual use.

increased pro-MMP-2 and pro-MMP-9 activity. Our results suggest that HIF-1 $\alpha$  accumulation may be involved in the increased MMP-2 and MMP-9 production in U937 cells exposed to Nano-Ni.

### Keywords

Metal nanoparticles; hypoxia inducible factor 1 $\alpha$ ; matrix metalloproteinases; human monocyte U937; tissue inhibitor of metalloproteinases

---

### Introduction

With the development of nanotechnology, a large number of transition metal nanoparticles, such as nano-sized nickel (Nano-Ni), are being developed and produced as new formulations with surface properties to meet novel demands. Nickel and its alloys have many commercial and industrial applications. Due to the special characteristics of Nano-Ni, including high levels of surface energy, high magnetism, high surface area, low melting point, and low burning point, it is widely used in magnetic tape, conduction paste, chemical catalysts, microfilters, gas-sensing equipment, light absorbance and sintering promoters (Zhang et al. 1998a, 1998b; Serita et al. 1999). Therefore, the population that is exposed to occupational and non-occupational Nano-Ni continues to increase. Our current knowledge about health effects of Nano-Ni is limited, but suggests that Nano-Ni may cause greater inflammatory response in lungs than that of standard-sized nickel particles (Std-Ni) (Zhang et al. 2003). Nanoparticles may also enter the blood circulation and translocate to extra-pulmonary tissues (Ferin et al. 1990; Takenaka et al. 2001; Nemmar et al. 2001, 2002; Oberdörster 2001; Oberdörster et al. 2002; Oberdörster and Utell 2002). The translocation of particles depends on the exposure route, dose, particle diameter, and surface chemical characteristics. Our previous results showed that metal nanoparticles (such as nickel and cobalt) could induce cytokine and NO release by blood neutrophils obtained from rats (Mo et al. 2008). This raises the intriguing possibility that nanoparticles could enter the circulation and produce direct or indirect effects on blood cells, such as monocytes or neutrophils. Recent studies in humans showed that exposure to nano-sized carbon altered peripheral blood leukocyte distribution and expression of adhesion molecules (Frampton et al. 2006).

Matrix metalloproteinases (MMPs) are a family of zinc-dependent endopeptidases that play an active role in regulating the extracellular matrix (Murphy et al. 1994; Parks and Shapiro 2001; Parks 2003; Greenlee et al. 2007). MMPs also play a key role in normal and pathological processes, including embryogenesis, wound healing, inflammation, arthritis, cardiovascular diseases and cancer (Murphy et al. 1994; Parks and Shapiro 2001; Parks 2003; Greenlee et al. 2007). In vertebrates, MMPs can be sub-grouped into five groups based on their primary protein structure and substrate specificity: collagenases, gelatinases, stromelysins, membrane type (MT)-MMPs and non-classified MMPs (Murphy et al. 1994; Greenlee et al. 2007). Among the MMPs, the 72 kDa gelatinase A (or MMP-2) and the 92 kDa gelatinase B (or MMP-9) are believed to be the critical enzymes for degrading type IV collagen, a major component of basement membrane (Murphy et al. 1994; Greenlee et al. 2007). It is believed that the secretion of gelatinases having specificity for type IV collagen

would endow endothelial cells with an advantage for degradation of the extracellular matrix and subsequent migration across the basement membrane. MMPs are often secreted in latent form and are usually activated after a small 10-kDa peptide is cleaved from the N-termini. MMPs can thus be recognized in both inactive (pro-MMPs) and active forms (MMPs) based on their different molecular weight (Greenlee et al. 2007). It is well known that regulation of MMPs may occur at multiple levels, either by gene transcription and synthesis of inactive pro-enzymes, post-translational activation of pro-enzymes, or via the interaction of secreted MMPs with their inhibitors called tissue inhibitor of metalloproteinases (TIMPs) (Murphy et al. 1994; Parsons et al. 1997; Oum'hamed et al. 2004). Our and other previous studies suggested that human monocytes, such as U937 cells, exposed to metal ions, such as  $\text{Co}^{2+}$ ,  $\text{Cr}^{3+}$  and  $\text{Ni}^{2+}$  or cobalt nanoparticles (Nano-Co) altered the activity of MMPs and TIMPs via protein tyrosine kinase (PTK) which was activated by oxidative stress (Luo et al. 2005; Perfetto et al. 2007; Wan et al. 2008). However, few studies have investigated the effects of nickel nanoparticles on alteration of MMPs/TIMPs expression or activities and the potential mechanisms involved in these effects.

Nickel is known to mimic hypoxia through activation of hypoxia inducible factor 1 $\alpha$  (HIF-1 $\alpha$ ) (Salnikow et al. 2002; Maxwell and Salnikow 2004). Hypoxia results in the accumulation and stabilization of HIF-1 $\alpha$ . Upon dimerization with another subunit of HIF, HIF-1 $\beta$ , HIF-1 binds to hypoxia response elements (HRE) in target genes, such as VEGF and MMPs, and activates them (Salnikow et al. 2002; Maxwell and Salnikow 2004). Several studies have shown that exposure to hypoxic stress resulted in MMPs modulation through activation of HIF-1 $\alpha$  (Milkiewicz and Haas 2005; Fujiwara et al. 2007; Misra et al. 2008). It was reported that exposure to nickel caused up- or down-regulation of many genes, and some up-regulated genes are HIF-1 $\alpha$ -dependent (Salnikow et al. 2002, 2003; Zhao et al. 2004; Davidson et al. 2003). Similar to hypoxia, disruption of prolyl hydroxylase activity has been shown to be one of the mechanisms for Ni-induced HIF-1 $\alpha$  stabilization (Salnikow et al. 2002, 2003; Davidson et al. 2003).

In the present study, we hypothesized that exposure to Nano-Ni would alter transcription and activity of MMP-2 and MMP-9 through activation of HIF-1 $\alpha$ . We first investigated whether exposure of U937 cells to Nano-Ni caused an alteration in the transcription of MMP-2, MMP-9 and their natural inhibitors, TIMP-1 and TIMP-2, and in the activity of pro-MMP-2 and pro-MMP-9. We then studied whether exposure to Nano-Ni resulted in HIF-1 $\alpha$  accumulation, and whether the increased MMP-2 and MMP-9 activity induced by Nano-Ni was regulated by activation of HIF-1 $\alpha$  pathway.

## Materials and methods

### Metal nanoparticles and their characterization

Nano-Ni and Nano-TiO<sub>2</sub> with a mean diameter of 20 nm and 28 nm were provided by INABATA and Co., Ltd, Vacuum Metallurgical Co., Ltd, Japan. The microstructure and composition of Nano-Ni and Nano-TiO<sub>2</sub> were characterized by transmission electron microscopy (TEM) (Hitach H-8000) and ancillary techniques including selected area electron diffraction (SAED) and energy-dispersive (X-ray) spectrometry (EDS). Nano-Ni and Nano-TiO<sub>2</sub> were dispersed in physiological saline and ultrasonicated for 30 min prior to

each experiment. The characterization of these nanoparticles has been summarized in Table I. Briefly, the specific surface area is 43.8 m<sup>2</sup>/g for Nano-Ni and 45.0 m<sup>2</sup>/g for Nano-TiO<sub>2</sub>. Nano-Ni is composed of 85–90% of metal nickel and 10–15% of NiO; Nano-TiO<sub>2</sub> is composed of 90% anatase and 10% rutile. The size of particles and agglomerates in cell culture medium (RPMI-1640) was 250 nm for Nano-Ni and 280 nm for Nano-TiO<sub>2</sub> which was measured by dynamic light scattering (DLS) and was also summarized in Table I.

The solubility of Nano-Ni and Nano-TiO<sub>2</sub> in 1 × PBS and cell culture medium (RPMI-1640) was measured as previously reported (Serita et al. 1999). In brief, five 30 mg samples of Nano-Ni or Nano-TiO<sub>2</sub> were suspended in 30 ml of 1 × PBS or RPMI-1640 medium, respectively. After shaking for 48 h in a water bath at 37° C, the samples were ultrasonicated for 30 min and then centrifuged at 12,000 *g* for 20 min. The supernatants were collected to determine the concentration of nickel or titanium ion by inductively coupled plasma-atomic emission spectrometry (ICP-AES). The results are shown in Table II.

### Chemicals and reagents

Monoclonal mouse anti-human HIF-1 $\alpha$  antibody was obtained from BD Transduction Laboratories (San Jose, CA, USA), horseradish peroxidase-conjugated goat anti-mouse IgG from Santa Cruz Biotechnology (Santa Cruz, CA, USA). Gelatin was purchased from Acros Organics (Morris Plains, NY, USA), MG-132 from Calbiochem (San Diego, CA, USA) and 17-allylamino-17-demethoxygeldanamycin (17-AAG) from Invivogen (San Diego, CA, USA). All other chemicals were purchased from Fisher Chemical (Pittsburgh, PA, USA) unless otherwise indicated. All chemicals used were of analytic grade.

### Cell culture and treatment

Human myelomonocytic U937 cells were obtained from American Type Culture Collection (ATCC) (Rockville, MD, USA) and cultured at 37° C in a 5% CO<sub>2</sub> atmosphere in RPMI 1640 medium (Mediatech, Inc., Manassas, VA, USA) containing 10% fetal bovine serum (FBS) (Mediatech), 100 U/ml penicillin and 100  $\mu$ g/ml streptomycin (Mediatech). U937 cells were exposed to Nano-Ni or Nano-TiO<sub>2</sub> at the doses and times indicated in each experiment. For MMP-2 and MMP-9 analysis, cells were cultured in 1% FBS for serum starvation for 24 h to minimize the selective activation of MMPs. In the studies to determine the effects of the specific inhibitors of HIF-1 $\alpha$  on the stimulation of MMP-2 and MMP-9 expression by Nano-Ni, U937 cells were pre-treated with 17-AAG (1  $\mu$ M) for 4 h prior to exposure to Nano-Ni. Unexposed U937 cells were served as negative controls.

In order to confirm that the bands observed on the gelatin zymography assay were MMP-2 and MMP-9, human fibrosarcoma cell line HT1080 was used. These cells are known to express high levels of MMP-2 and MMP-9 (Zeng and Briske-Anderson 2005). HT1080 was obtained from ATCC and was grown in Dulbecco's Modification of Eagle's Medium (DMEM) (Mediatech) supplemented with 10% FBS, 100 U/ml penicillin and 100  $\mu$ g/ml streptomycin.

HT1080 cells were cultured in serum-free DMEM for two days, and the supernatants were collected and used as a molecular weight marker for MMP-2, pro-MMP-2, MMP-9 and Pro-

MMP-9 as described elsewhere (Togawa et al. 1999; Dagnell et al. 2007; Das et al. 2008; Wan et al. 2008).

### Cytotoxicity assay

The cytotoxicity of Nano-Ni or Nano-TiO<sub>2</sub> in U937 cells was determined by both CellTiter 96 AQueous Non-Radioactive Cell Proliferation Assay (MTS assay) (Promega, Madison, WI, USA) and alamarBlue™ assay (AbD Serotec, Oxford, UK) according to the manufacturer's instruction. MTS assay is based on the cellular conversion of a tetrazolium compound (MTS) into a formazan product that is soluble in tissue culture medium. The quantity of formazan product was measured by the amount of absorbance at 490 nm which is directly proportional to the number of living cells in culture. Briefly,  $2 \times 10^4$  U937 cells in 100  $\mu$ l RPMI 1640 medium were seeded into each well of 96-well plates and incubated overnight. Then cells were treated with various concentrations of Nano-Ni or Nano-TiO<sub>2</sub> for 24 h. 20  $\mu$ l of the combined MTS/PMS (phenazine methosulfate) solution was added to each well of the plate. After incubation at 37° C for 3 h, the absorbance at 490 nm was measured with a multidetection microplate reader (Synergy HT, BioTek, Winooski, VT, USA). In order to eliminate the potential effects of metal nanoparticles on optical properties, medium with metal nanoparticles at each dose, but without cells were used as background and their A<sub>490</sub> readings were subtracted from the experimental groups. Another method, alamarBlue™ assay, is a colorimetric/fluorometric method for determining the number of metabolically active cells through oxidation-reduction indicator. This method was performed as in our previous study (Yu et al. 2010).

### RNA isolation and reverse transcription-polymerase chain reaction (RT-PCR)

Total RNAs were isolated from cultured cells using TRIZOL Reagent (Sigma, St Louis, MO, USA) and quantified by measuring absorbance (260 nm). cDNA was synthesized from 2.0  $\mu$ g of total RNA using M-MLV reverse transcriptase (Promega, Madison, WI, USA) and oligo (dT)<sub>18</sub> (Sigma). A total of 1  $\mu$ l of cDNA, 1  $\mu$ l of 5  $\mu$ M each primer, and 1.25 units of Taq polymerase (Promega, Madison, WI, USA) were used in each PCR reaction at a final volume of 25  $\mu$ l. PCR reaction was performed on a Mastercycler (Eppendorf) using 35 cycles at 94° C for 45 s, at 62° C for 45 s, and at 72° C for 45 s for MMP-2 and MMP-9; 25 cycles (GAPDH) and 30 cycles (TIMP-1 and TIMP-2) at 94° C for 45 s, at 58.5° C for 45 s, and at 72° C for 45 s for TIMP-1, TIMP-2 and GAPDH. The primers for human MMP-9 were: forward 5'-CGG TGA TTG ACG ACG CCT TTG C-3' and reverse 5'-CGC TGT CAA AGT TCG AGG TGG TA-3'; for human MMP-2 were: forward 5'-ATT TGG CGG ACT GTG ACG-3' and reverse 5'-GCT TCA GGT AAT AGG CAC-3'; for human TIMP-1 were: forward 5'-AAT TCC GAC CTC GTC ATC AG-3' and reverse 5'-GTT TGC AGG GGA TGG ATA AA-3'; for human TIMP-2 were: forward 5'-CTG GAC GTT GGA GGA AAG AA-3' and reverse 5'-GTC GAG AAA CTC CTG CTT GG-3'; for human GAPDH were: forward 5'-AGC CAC ATC GCT CAG ACA C-3' and reverse 5'-TGG ACT CCA CGA CGT ACT C-3'. Amplified fragments were analyzed using 1.2% agarose gel, and photographed (Polaroid, 667) on an ultraviolet screen. Pictures were scanned and analyzed by NIH Image J software. Intensities of MMP-2, MMP-9, TIMP-1 and TIMP-2 products were then normalized by that of human GAPDH to obtain the relative densities.

### Gelatin zymography assay

MMP-2 and MMP-9 activities were measured by gelatin zymography as previously described (Mo et al. 2009; Wan et al. 2008). U937 cells were cultured in six-well plates ( $1 \times 10^6$  cells/well) in 1 ml RPMI1640 containing 1% FBS for 24 h before exposure to Nano-Ni or Nano-TiO<sub>2</sub>. The conditioned media were subjected to gelatin zymography under non-reducing conditions on 10% SDS-PAGE copolymerized with 0.5 mg/ml gelatin. After electrophoresis, the gels were washed twice with 50 mM Tris-HCl (pH 7.5) containing 2.5% Triton X-100 (Sigma) for 30 min each time to remove SDS. Then the gels were incubated in development buffer (pH 7.4) containing 10 mM CaCl<sub>2</sub> and 0.05% Brij solution (Bio-Rad, Hercules, CA, USA) at 37° C overnight. The lysed regions indicating gelatinase activity were visualized as clear bands after staining with 0.1% Coomassie Brilliant Blue R-250 (Bio-Rad, Hercules, CA, USA) and then destaining. Enzyme activity was quantified by scanning densitometry as described above.

### Protein extraction and immunoblot analysis

Nuclear proteins were used to detect the alteration of HIF-1 $\alpha$  expression after U937 cells were treated with Nano-Ni or Nano-TiO<sub>2</sub>. Nuclear extracts were prepared using NE-PER<sup>®</sup> Nuclear and Cytoplasmic Extraction Reagent (Thermo Fisher Scientific, Rockford, IL, USA) according to the manufacturer's instructions. 100  $\mu$ g of protein was loaded into each lane, separated on 10% SDS-PAGE and transferred to polyvinylidene difluoride (PVDF) membrane (Bio-Rad). The non-specific binding sites were blocked with 5% milk/TBST (50 mM Tris-HCl, 140 mM NaCl, 0.05% Tween-20, pH 7.2) for 2 h at room temperature. The membrane was incubated with anti-HIF-1 $\alpha$  antibody (1:1000) at 4° C overnight and rinsed with TBST three times. Immunoreactive bands were detected by goat anti-mouse horseradish peroxidase conjugated secondary antibody (1:2000) and enhanced chemiluminescence substrates (GE Healthcare, Buckinghamshire, UK). Equal protein loading was verified by Coomassie Brilliant Blue staining.

### Statistical analysis

Values were presented as mean  $\pm$  SD. For dose-response studies, differences among groups were evaluated with two-way analysis of variance; if the F-value was significant, groups were then compared at each dose by one-way analysis of variance (ANOVA) followed by Dunnett's *t*-test. A value of  $P < 0.05$  was considered significant. Statistical analyses were carried out using SigmaStat software (Jandel Scientific, San Raphael, CA, USA).

## Results

### Cytotoxic effects of Nano-Ni and Nano-TiO<sub>2</sub> on U937 cells

U937 cells were exposed to various concentrations of Nano-Ni or Nano-TiO<sub>2</sub> for 24 h, and cell viability was measured by both MTS assay and alamarBlue<sup>trade</sup> assay as described above. Exposure of U937 cells to Nano-Ni at 60  $\mu$ g/ml and beyond caused significant cell death by MTS assay, while exposure to 30  $\mu$ g/ml or less of Nano-Ni did not cause significant cell death (Figure 1A). However, exposure of U937 cells to any doses from 0 to 60  $\mu$ g/ml of Nano-TiO<sub>2</sub> did not cause any cytotoxic effects (Figure 1A). These results were further



confirmed by alamarBlue™ assay (Figure 1B). In all following experiments, non-toxic doses were chosen to observe the effects of Nano-Ni on U937 cells.

### **Exposure of U937 cells to Nano-Ni caused increased mRNA expression of MMP-2 and MMP-9 and increased activity of pro-MMP-2 and pro-MMP-9**

To investigate the effects of Nano-Ni or Nano-TiO<sub>2</sub> on MMP-2 and MMP-9 mRNA expression, U937 cells were treated with various concentration of Nano-Ni or Nano-TiO<sub>2</sub>. The results showed a dose-response increase in MMP-2 and MMP-9 mRNA levels after cells were exposed to 10 and 30 µg/ml of Nano-Ni for 24 h, whereas Nano-TiO<sub>2</sub> did not induce any significant changes (Figure 2A, 2B). Our results also showed a time-response increase in MMP-2 and MMP-9 mRNA levels after exposure to 30 µg/ml of Nano-Ni for 0, 6, 12, 24 and 48 h (Figure 3A, 3B). Again, Nano-TiO<sub>2</sub> did not cause any increase in the MMP-2 and MMP-9 mRNA levels (data not shown).

We also evaluated the activity of pro-MMP-2 and pro-MMP-9 in U937 cells with exposure to Nano-Ni or Nano-TiO<sub>2</sub> by gelatin zymography assay. The results showed a dose-response increase in pro-MMP-2 and pro-MMP-9 activity in the conditioned media from U937 cells exposed to Nano-Ni for 24 h (Figure 4A, 4B). In the time course studies, the results showed that exposure to 30 µg/ml of Nano-Ni significantly increased pro-MMP-2 and pro-MMP-9 activity in U937 cells at 12, 24 and 48 h as compared with those in the control, and the activities reached a peak after 24 h exposure (Figure 5A, 5B). Consistent with the RT-PCR results, exposure to Nano-TiO<sub>2</sub> did not cause dose-response (Figure 4) or time-response (data not shown) increase in the pro-MMP-2 and pro-MMP-9 activity.

### **Effects of Nano-Ni on TIMP-1 and TIMP-2 mRNA expression**

The mRNA expression of TIMP-1 and TIMP-2 was determined in U937 cells exposed to metal nanoparticles. Our results showed that exposure of U937 cells to Nano-Ni for 24 h caused a dose-response increase in TIMP-1 mRNA expression, reaching statistically significant increase when cells were exposed to as low as 10 µg/ml of Nano-Ni (Figure 6A, 6B).

Exposure to Nano-TiO<sub>2</sub> did not have any effects on TIMP-1 mRNA expression (Figure 6A, 6B). Figure 7 showed that TIMP-1 mRNA expression increased when U937 cells were treated with 30 µg/ml of Nano-Ni for 12, 24 and 48 h. Treatment with Nano-TiO<sub>2</sub> did not cause any increase in TIMP-1 mRNA expression (data not shown). Exposure of U937 cells to either Nano-Ni or Nano-TiO<sub>2</sub> did not cause any change in TIMP-2 mRNA expression (data not shown).

### **Exposure of U937 cells to Nano-Ni caused HIF-1α accumulation**

To examine whether exposure to Nano-Ni or Nano-TiO<sub>2</sub> caused HIF-1α accumulation, U937 cells were treated with various doses of metal nanoparticles for different times, and HIF-1α expression was determined by Western blot. The results showed that exposure to 10 and 30 µg/ml of Nano-Ni for 24 h caused significant HIF-1α accumulation (Figure 8). There was also a time-dependent increase in HIF-1α accumulation in U937 cells exposed to 30 µg/ml of Nano-Ni (Figure 9). However, exposure to Nano-TiO<sub>2</sub> did not result in a dose-

dependent (Figure 8) or time-dependent (data not shown) increase in the HIF-1 $\alpha$  accumulation.

### **Effects of heat-shock protein 90 (Hsp90) inhibitor, 17-AAG, on Nano-Ni-induced MMP expression and activity in U937 cells**

Hsp90, a molecular chaperone that protects client proteins from misfolding and degradation (Neckers and Ivy 2003; Whitesell and Lindquist 2005), is essential for HIF-1 activation in hypoxia and can also protect HIF-1 $\alpha$  from degradation (Minet et al. 1999). To examine the role of HIF-1 $\alpha$  in the Nano-Ni-induced MMP expression and activity, 17-AAG, an Hsp90 inhibitor, was used to pre-treat U937 cells prior to exposure to Nano-Ni. Our results showed that 17-AAG significantly inhibited Nano-Ni induced HIF-1 $\alpha$  accumulation (Figure 10). A proteasome inhibitor, MG132 (1  $\mu$ M), was used as positive control for HIF-1 $\alpha$  (Figure 10) since MG132 can inhibit HIF-1 $\alpha$  from proteasomal degradation. To investigate the role of HIF-1 $\alpha$  in Nano-Ni-induced MMP and TIMP expression, U937 cells were pretreated with 17-AAG for 4 h, followed by 30  $\mu$ g/ml of Nano-Ni treatment for another 24 h. RT-PCR results showed that pre-treatment with 17-AAG significantly inhibited MMP-2 and MMP-9 gene expression induced by Nano-Ni (Figure 11A, 11B). The results were further confirmed by gelatin zymography analysis which showed that pre-treatment with 17-AAG attenuated the activity of pro-MMP-2 and pro-MMP-9 (Figure 12A, 12B). Furthermore, pre-treatment with 17-AAG also attenuated the increased expression of TIMP-1 caused by exposure to Nano-Ni (Figure 13A, 13B).

### **Discussion and conclusion**

A previous study showed that inhaled nano-sized particles penetrate rapidly through the epithelium, reach the endothelium and enter the bloodstream (Frampton et al. 2006). This translocation of nanoparticles may result in adverse effects on blood cells such as monocytes/macrophages. The studies of the potential biological and toxic effects of nickel nanoparticles are limited but suggest that they may exert adverse effects by passage through epithelia and tissue membranes. Monocytes/macrophages are possible target for metal nanoparticles when they are translocated from the lungs to the circulatory system, thus we studied whether some metal nanoparticles, such as Nano-Ni and Nano-TiO<sub>2</sub> can activate monocytes/macrophages and result in potential pathological or toxic responses. In this study, the alteration of expression and secretion of two gelatinases, MMP-2 and MMP-9, and their specific tissue inhibitors, TIMP-1 and TIMP-2, in human U937 monocytes exposed to Nano-Ni and Nano-TiO<sub>2</sub> was determined. We also explored the possible mechanisms involved in the regulation of MMP expression and activity after exposure to these metal nanoparticles.

The results showed a dose-response cytotoxic effect on U937 cells after exposure to Nano-Ni at concentrations ranging from 0–60  $\mu$ g/ml. Exposure to Nano-Ni at concentrations 60  $\mu$ g/ml and beyond caused significant cytotoxic effects. However, there were no cytotoxic effects on U937 cells with exposure to Nano-TiO<sub>2</sub> in all experimental doses. Although our in vitro results can not be used to predict the degree of human health effects at these concentrations, or to determine the real human being exposure to nanoparticles that might be comparable to these dose-response studies, these dose-response studies provide a basis for



planning organ toxicological studies and further mechanistic studies. Choosing the doses that are lower than the cytotoxic dose can help to identify potential toxic effects of nanoparticles that are not due to cytotoxicity (Mo et al. 2009).

Under normal physiological conditions, a balance between MMPs and TIMPs regulates enzyme activity. An excessive or inappropriate expression of MMPs and/or decrease in TIMPs production might contribute to different pathological conditions, such as inflammation, altered wound healing, invasion of cancer cells and infectious diseases (Elkington et al. 2005; Cauwe et al. 2007). Regulation of MMPs occurs at both the transcriptional level and after secretion from a variety of cells, such as macrophages, fibroblasts, and smooth muscle cells. Therefore, understanding how metal nanoparticles induce changes in the MMP/TIMP system that result in matrix breakdown may lead to interventions that delay or prevent potential health effects of metal nanoparticles. In the present study, we determined the MMP-2 and MMP-9 expression in U937 cells exposed to Nano-Ni or Nano-TiO<sub>2</sub> by using RT-PCR and the pro-MMP-2 and pro-MMP-9 activity by using gelatin zymography assay. Our results demonstrated a dose- and time-response increase in MMP-2 and MMP-9 expression and pro-MMP-2 and pro-MMP-9 activity with exposure to Nano-Ni. Activation of MMP-2 and MMP-9 is a complex process, which is further regulated by the action of TIMP-1 and TIMP-2. Therefore, we also investigated the transcription levels of TIMP-1 and TIMP-2. Our results demonstrate that exposure to Nano-Ni also up-regulated TIMP-1 mRNA expression in U937 cells exposed to Nano-Ni. However, neither Nano-Ni nor Nano-TiO<sub>2</sub> exposure led to the alteration of TIMP-2 expression. Though TIMPs are believed the inhibitors of MMPs, the activation of TIMP-1 is not always strictly related to its function as a MMP inhibitor (Camarota et al. 2006). Upregulation of some TIMPs were also reported to be an adaptive response that may contribute to the creation of a sub-population of cells that are apoptotically resistant but genetically damaged, predisposing to mutagenesis (Camarota et al. 2006). The effects of Nano-Ni on the upregulation of MMP-2 and MMP-9 expression and pro-MMP-2 and pro-MMP-9 activity may lead to an imbalance in the MMP/TIMP system which may result in net matrix breakdown.

Oxidative stress, pro-inflammatory cytokines, and nitric oxide have been shown to play important roles in the regulation of both MMP and TIMP expression in several types of cells, including hepatic stellate cells (Galli et al. 2005), human monocytes (Lu and Wahl 2005; Wan et al. 2008), and human coronary smooth muscle cells (Valentin et al. 2005). Other transcription factors, such as HIF-1 may also be involved in the regulation of MMP/TIMP expression or activity. HIF-1 is a key transcription factor regulating the cellular oxygen homeostasis. It is composed of HIF-1 $\alpha$  and HIF-1 $\beta$ , both of which belong to the PAS family of basic helix-loop-helix transcription factors (Wang et al. 1995). HIF-1 $\alpha$  is produced or activated in response to hypoxia (Wang and Semenza 1993a, 1993b, Wang et al. 1995; Yamashita et al. 2001), whereas HIF-1 $\beta$  protein is constitutively present regardless of oxygen tension (Liu et al. 2007). Under normoxia, HIF-1 $\alpha$  subunit is rapidly degraded by prolyl hydroxylase (PHD), the von Hippel-Lindau (VHL)/Elongin-C/Elongin-B E3 ubiquitin ligase complex, and the proteasome (Maxwell et al. 1999). However, under hypoxic condition, HIF-1 $\alpha$  translocates from the cytosol to the nucleus and heterodimerizes with HIF-1 $\beta$  to form the active HIF-1 protein, binding and activating hypoxia responsive genes,

such as VEGF and MMPs. Inhibition of Hsp90 caused O<sub>2</sub>/PHD/VHL-independent degradation of HIF-1 $\alpha$ . Hsp90 competes with receptor of activated protein kinase C (RACK1) for binding to the PAS A-domain for HIF-1 $\alpha$ . Hsp90 inhibition leads to increased RACK1 binding and recruitment of the Elongin C ubiquitin-ligase complex that mediates ubiquitination and proteasomal degradation of HIF-1 $\alpha$  (Liu et al. 2007). Previous *in vitro* and *in vivo* studies have clearly shown that exposure to nickel caused HIF-1 $\alpha$  accumulation (Salnikow et al. 2002, 2003; Davidson et al. 2003; Zhao et al. 2004). Our results also demonstrated a dose- and time-related increase in the accumulation of HIF-1 $\alpha$  after exposure to non-toxic doses of Nano-Ni. It has been reported that hypoxia can induce MMP expression in endothelial cells, cardiac fibroblasts, macrophages and breast cancer cells (Rajagopalan et al. 1996; Belkhiri et al. 1997; Siwik et al. 2001; Zhang et al. 2002; Hemmerlein et al. 2004). This raises an interesting question, whether HIF-1 $\alpha$  pathway is involved in the Nano-Ni-induced MMP expression and activity. To investigate the role of HIF-1 $\alpha$  in Nano-Ni-induced MMP/TIMP expression imbalance, the Hsp90 inhibitor 17-AAG was used to pre-treat U937 cells. Our results clearly showed that pre-treatment with 17-AAG significantly inhibited Nano-Ni-induced up-regulation of MMP-2 and MMP-9 expression, activity of pro-MMP-2 and pro-MMP-9, and up-regulation of TIMP-1 expression. The results suggest that HIF-1 $\alpha$  may be involved not only in the regulation of MMPs, but also in the regulation of TIMP-1, which is consistent with previous studies (Haorah et al. 2007; Ho et al. 2007; Shi et al. 2007). shRNA targeting against HIF-1 $\alpha$  mRNA effectively silenced HIF-1 $\alpha$ , inhibiting the hypoxia-induced up-regulation of TIMP-1 (Yang et al. 2006). Unlike TIMP-1, TIMP-2 was not induced by exposure to Nano-Ni. Regulation of MMPs and TIMPs expression or activity is complex process, which is regulated by many factors, such as oxidative stress, growth factors, cytokines, et al. In the present study, our results clearly demonstrated that exposure to Nano-Ni caused HIF-1 $\alpha$  accumulation, MMP-2, MMP-9 and TIMP-1 up-regulation. Though it is difficult to identify whether exposure to Nano-Ni caused increased MMPs and TIMPs expression through the HIF-1 $\alpha$  pathway or whether Nano-Ni-induced changes in all these parameters at the same time, pretreatment U937 cells with the Hsp90 inhibitor, 17-AAG, prior to treatment with Nano-Ni resulted in the suppression of HIF-1 $\alpha$  as well as MMP-2 and MMP-9. Our results also showed that pre-treatment cells with 17-AAG did not alter the transcription expression or activity of MMP-2 and MMP-9, which may exclude the potential independently effects of 17-AAG. Therefore, Nano-Ni-induced accumulation of HIF-1 $\alpha$  is at least partly involved in the activation of MMPs.

In conclusion, we have demonstrated that exposure to Nano-Ni enhanced the transcription and activity of MMP-2 and MMP-9 in U937 cells. The HIF-1 $\alpha$  signaling pathway may be involved in this process via Nano-Ni-induced hypoxia. However, the detailed mechanisms need to be further studied. These data provide valuable clues to the potential health effects of metal nanoparticle exposure.

## Acknowledgments

The contents of this article do not necessarily reflect the views of HEI, or its sponsors, nor do they necessarily reflect the views and policies of the EPA or motor vehicle and engine manufacturers.

This work was partly supported by American Lung Association (RG-872-N), American Heart Association (086576D), KSEF-1686-RED-11, Health Effects Institute (4751-RFA-05-2/06-12), CTSPGP 20018 from University of Louisville, T32-ES011564 and ES01443.

Some of research described in this article was conducted under contract to the Health Effects Institute (HEI), an organization jointly founded by the United States Environmental Protection Agency (EPA) (Assistance Award No. R-8281101) and certain motor vehicle and engine manufacturers.

## References

- Belkhir A, Richars C, Whaley M, McQuwwn SA, Orr FW. Increased expression of activated matrix metalloproteinase-2 by human endothelial cells after sublethal H<sub>2</sub>O<sub>2</sub> exposure. *Lab Invest.* 1997; 77:533–539. [PubMed: 9389796]
- Cammarota M, Lamberti M, Masella L, Galletti P, De Rosa M, Sannolo N, Giuliano M. Matrix metalloproteinases and their inhibitors as biomarkers for metal toxicity in vitro. *Toxicol in Vitro.* 2006; 20:1125–1132. [PubMed: 16581223]
- Cauwe B, Van den Steen PE, Opdenakker G. The biochemical, biological, and pathological kaleidoscope of cell surface substrates processed by matrix metalloproteinases. *Crit Rev Biochem Mol Biol.* 2007; 42:113–185. [PubMed: 17562450]
- Davidson T, Salnikow K, Costa M. Hypoxia inducible factor-1 alpha-independent suppression of aryl hydrocarbon receptor-regulated genes by nickel. *Mol Pharmacol.* 2003; 64:1485–1493. [PubMed: 14645679]
- Dagnell C, Kemi C, Klominek J, Eriksson P, Skold M, Eklund A, Grunewald J, Hoglund CO. Effects of neurotrophins on human bronchial smooth muscle cell migration and matrix metalloproteinase-9 secretion. *Translational Res.* 2007; 150:303–310.
- Das S, Banerji A, Frei E, Chatterjee A. Rapid expression and activation of MMP-2 and MMP-9 upon exposure of human breast cancer cell (MCF-7) to fibronectin in serum free medium. *Life Sci.* 2008; 82:467–476. [PubMed: 18243246]
- Elkington PT, O' Kane CM, Friedland JS. The paradox of matrix metalloproteinases in infectious disease. *Clin Exp Immunol.* 2005; 142:12–20. [PubMed: 16178851]
- Ferin J, Oberdöster G, Penney D. Increased pulmonary toxicity of ultrafine? I. Particle clearance, translocation, morphology. *J Aerosol Sci.* 1990; 21:381–384.
- Frampton MW, Stewart JC, Oberdöster G, Morrow PE, Chalupa D, Pietropaoli AP, Frasier LM, Dpeers DM, Huang LS, Utell MJ. Inhalation of ultrafine particles alters blood leukocytes expression of adhesion molecules in humans. *Environ Health Perspect.* 2006; 114:51–58.
- Fujiwara S, Nakagawa K, Harada H, Nagato S, Furukawa K, Teraoka M, Seno T, Oka K, Iwata S, Ohnishi T. Silencing hypoxia-inducible factor-1alpha inhibits cell migration and invasion under hypoxic environment in malignant gliomas. *Int J Oncol.* 2007; 30:793–802. [PubMed: 17332917]
- Galli A, Svegliati-Baroni G, Milani S, Ridolfi F, Salzano R, Tarocchi M, Crappone C, Pellegrini D, Benedetti A, Surrenti C, Casini A. Oxidative stress stimulates proliferation and invasiveness of hepatic stellate cells via a MMP2-mediated mechanism. *Hepatology.* 2005; 41:1074–1084.
- Greenlee KJ, Werb Z, Kheradmand F. Matrix metalloproteinases in lung: Multiple, multifarious, and multifaceted. *Physiol Res.* 2007; 87:69–98.
- Haorah J, Ramirez SH, Schall K, Smith S, Pandya R, Persidsky Y. Oxidative stress activates protein kinase and matrix metalloproteinases leading to blood-brain barrier dysfunction. *J Neurochem.* 2007; 101:566–576. [PubMed: 17250680]
- Hemmerlein B, Johanns U, Halbfass J, Bottcher T, Heuser M, Radzun HJ, Thelen P. The balance between MMP-2/-9 and TIMP-1/-2 is shifted towards MMP in renal cell carcinomas and can be further disturbed by hydrogen peroxide. *Int J Oncol.* 2004; 24:1069–1076. [PubMed: 15067327]
- Ho FM, Liu SH, Lin WW, Liao CS. Opposite effects of high glucose on MMP-2 and TIMP-2 in human endothelial cells. *J Cell Biochem.* 2007; 101:442–450. [PubMed: 17203468]
- Luo L, Petit A, Antoniou J, Zukor DJ, Huk OL, Liu RCW, Winnik FM, Mwale F. Effect of cobalt and chromium ions on MMP-1, TIMP-1 and TNF-a gene expression in human U937 macrophages: A role of tyrosine kinases. *Biomaterials.* 2005; 26:5587–5593. [PubMed: 15878362]

- Liu YV, Baek JH, Zhang H, Diez R, Cole RN, Semenza GL. RACK1 competes with HSP90 for binding to HIF-1 $\alpha$  and is required for O(2)-independent and HSP90 inhibitor-induced degradation of HIF-1 $\alpha$ . *Mol Cell*. 2007; 25:207–217. [PubMed: 17244529]
- Lu Y, Wahl LM. Oxidative stress augments the production of matrix metalloproteinase-1, cyclooxygenase-2, and prostaglandin E2 through enhancement of NF- $\kappa$ B activity in lipopolysaccharide-activated human primary monocytes. *J Immunol*. 2005; 175:5423–5429. [PubMed: 16210649]
- Maxwell PH, Wiesener MS, Chang GW, Clifford SC, Vaux EC, Cockman ME, Wykoff CC, Pugh CW, Maher ER, Ratcliffe PJ. The tumor suppressor protein VHL targets hypoxia-inducible factors for oxygen-dependent proteolysis. *Nature*. 1999; 399:271–275. [PubMed: 10353251]
- Maxwell P, Salnikow K. HIF-1: An oxygen and metal responsive transcription factor. *Cancer Biol Ther*. 2004; 3:29–35. [PubMed: 14726713]
- Milkiewicz M, Haas TL. Effect of mechanical stretch on HIF-1{ $\alpha$ } and MMP-2 expression in capillaries isolated from overloaded skeletal muscles: Laser capture microdissection study. *Am J Physiol Heart Circ Physiol*. 2005; 289:H1315–1320. [PubMed: 15894575]
- Minet E, Mottet D, Michel G, Roland I, Raes M, Remacle J, Michiels C. Hypoxia-induced activation of HIF-1: Role of HIF-1 $\alpha$ -Hsp90 interaction. *FEBS Lett*. 1999; 460:251–256. [PubMed: 10544245]
- Misra S, Fu AA, Rajan DK, Juncos LA, McKusick MA, Bjarnason H, Mukhopadhyay D. Expression of hypoxia inducible factor-1  $\alpha$ , macrophage migration inhibition factor, matrix metalloproteinase-2 and -9, and their inhibitors in hemodialysis grafts and arteriovenous fistulas. *J Vasc Interv Radiol*. 2008; 19:252–259. [PubMed: 18341958]
- Mo Y, Zhu X, Hu X, Tollerud DJ, Zhang Q. Cytokine and NO release from peripheral blood neutrophils after exposure to metal nanoparticles: In vitro and ex vivo studies. *Nanotoxicology*. 2008; 2:79–87.
- Mo Y, Wan R, Chien S, Tollerud DJ, Zhang Q. Activation of endothelial cells after exposure to ambient ultrafine particles: the role of NADPH oxidase. *Toxicol Appl Pharmacol*. 2009; 236(2): 183–193. [PubMed: 19371610]
- Murphy G, Willenbrock F, Crabbe T, O’Shea M, Ward R, Atkinson S, O’Connell J, Docherty A. Regulation of matrix metalloproteinase activity. *Ann NY Acad Sci*. 1994; 994(732):31–41.
- Neckers L, Ivy SP. Heat shock protein 90. *Curr Opin Oncol*. 2003; 25:419–424.
- Nemmar A, Vanbilloen H, Hoylaerts MF, Hoet PHM, Verbruggen A, Nemery B. Passage of intratracheally instilled ultrafine particles from the lung into the systemic circulation in hamsters. *Am J Respir Crit Care Med*. 2001; 164:1665–1668. [PubMed: 11719307]
- Nemmar A, Hoet PHM, Vanquickenborme B, Dinsdale D, Thomeer M, Hoylaerts MF, Vanbilloen H, Mortelmans L, Nemery B. Passage of inhaled particles into the blood circulation in human. *Circulation*. 2002; 105:411–414. [PubMed: 11815420]
- Oberdörster G. Pulmonary effects of inhaled ultrafine particles. *Int Arch Occup Environ Heal*. 2001; 74:1–8.
- Oberdörster G, Sharp Z, Atudorei V, Elder A, Gelein R, Lunts A, Kreyling W, Cox C. Extra-pulmonary translocation of ultrafine carbon particles following whole-body inhalation exposure rats. *J Toxicol Environ Health A*. 2002; 65:1531–1543. [PubMed: 12396867]
- Oberdörster G, Utell MJ. Ultrafine particles in the urban air: To the respiratory tract – and beyond? *Environ Heal Perspect*. 2002; 110:A440–441.
- Oum’hamed Z, Garnotal R, Josset Y, Trenteseaux C, Lauren-Maquin D. Matrix metalloproteinases MMP-2, -9 and tissue inhibitors TIMP-1, -2 expression and secretion by primary human osteoblast cells in response to titanium, zirconia, and alumina ceramics. *J Biomed Mater Res*. 2004; 68A: 114–122.
- Parsons SL, Watson SA, Brown PD, Collins HM, Steele RJ. Matrix metalloproteinase. *Br J Surg*. 1997; 84:160–166. [PubMed: 9052425]
- Parks WC, Shapiro SD. Matrix metalloproteinases in lung biology. *Respir Res*. 2001; 2:10–19. [PubMed: 11686860]
- Parks WC. Matrix metalloproteinases in lung repair. *Eur Respir J*. 2003; (Suppl. 44):36s–38s.

- Perfetto B, Lamberti M, Giuliano MT, Canozo N, Cammarota M, Baroni A. Analysis of the signal transduction pathway of nickel-induced matrix metalloproteinase-2 expression in human keratinocytes in vitro: Preliminary findings. *J Gut Pathol.* 2007; 34:441–447.
- Rajagopalan S, Meng XP, Ramasamy S, Harrison DG, Galis ZS. Reactive oxygen species produced by macrophage-derived foam cells regulate the activity of vascular matrix metalloproteinases in vitro. Implications for atherosclerotic plaque stability. 1996; 98:2572–2579.
- Salnikow K, Davidson T, Costa M. The role of hypoxia-inducible signaling pathway in nickel carcinogenesis. *Environ Health Perspect.* 2002; 110(Suppl. 5):831–834. [PubMed: 12426141]
- Salnikow K, Davidson T, Zhang Q, Chen LC, Su W, Costa M. The involvement of hypoxia-inducible transcription factor-1-dependent pathway in nickel carcinogenesis. *Cancer Res.* 2003; 63:3524–3530. [PubMed: 12839937]
- Serita F, Kyono H, Seki Y. Pulmonary clearance and lesions in rats after a single inhalation of ultrafine metallic nickel at dose levels comparable to the threshold limit value. *Ind Health.* 1999; 37:353–363. [PubMed: 10547950]
- Shi YF, Fong CC, Zhang Q, Cheung PY, Tzang CH, Wu RS, Yang M. Hypoxia induces the activation of human hepatic stellate cells LX-2 through TGF-beta signaling pathway. *FEBS Lett.* 2007; 581:203–210. [PubMed: 17187782]
- Siwik DA, Pagano PJ, Colucci WS. Oxidative stress regulates collagen synthesis and matrix metalloproteinase activity in cardiac fibroblasts. *Am J Physiol Cell Physiol.* 2001; 280:C53–60. [PubMed: 11121376]
- Takenaka S, Karg E, Roth C, Schulz H, Ziesenis A, Heinzmann U, Schramel P, Heyder J. Pulmonary and systemic distribution of inhaled ultrafine silver particles in rats. *Environ Health Perspect.* 2001; 109(Suppl. 4):547–551.
- Togawa D, Koshino T, Saito T, Takagi T, Machida J. Highly activated matrix metalloproteinase-2 secreted from clones of metastatic lung nodules of nude mice injected with human fibrosarcoma HT1080. *Cancer Letter.* 1999; 146:25–33.
- Valentin F, Bueb JL, Kieffer P, Tschirhart E, Atkinson J. Oxidative stress activates MMP-2 in cultured human coronary smooth muscle cells. *Fundam Clin Pharmacol.* 2005; 19:661–667. [PubMed: 16313278]
- Wan R, Mo Y, Zhang X, Chien S, Tollerud DJ, Zhang Q. Matrix metalloproteinase-2 and -9 are induced differently by metal nanoparticles in human monocytes: The role of oxidative stress and protein tyrosine kinase activation. *Toxicol Appl Pharmacol.* 2008; 233:276–285. [PubMed: 18835569]
- Wang GL, Semenza GL. General involvement of hypoxia-inducible factor 1 in transcriptional response to hypoxia. *Proc Natl Acad Sci USA.* 1993a; 90:4304–4308. [PubMed: 8387214]
- Wang GL, Semenza GL. Characterization of hypoxia-inducible factor 1 and regulation of DNA binding activity by hypoxia. *J Biol Chem.* 1993b; 268:21513–21518. [PubMed: 8408001]
- Wang GL, Jiang BH, Rue EA, Semenza GL. Hypoxia-inducible factor 1 is a basic-helix-loop-helix-PAS heterodimer regulated by cellular O<sub>2</sub> tension. *Proc Natl Acad Sci USA.* 1995; 92:5510–5514. [PubMed: 7539918]
- Whitesell L, Lindquist SL. HSP90 and the chaperoning of cancer. *Nat Rev Cancer.* 2005; 5:761–772. [PubMed: 16175177]
- Yamashita K, Discher DJ, Hu J, Bishopric NH, Webster KA. Molecular regulation of the endothelin-1 gene by hypoxia. Contributions of hypoxia-inducible factor-1, activator protein-1, GATA-2, AND p300/CBP. *J Biol Chem.* 2001; 276:12645–12653. [PubMed: 11278891]
- Yang C, Zeng S, Lv M. Effect of shRNA inhibiting HiF1-alpha gene on TIMP1 expression in RPE cells. *J Huazhong Univ Sci Technolog Med Sci.* 2006; 26:133–136. [PubMed: 16711028]
- Yu M, Mo Y, Wan R, Chien S, Zhang X, Zhang Q. Regulation of plasminogen activator inhibitor-1 expression in endothelial cells with exposure to metal nanoparticles. *Toxicol Lett.* 2010; 195:82–89. [PubMed: 20171267]
- Zeng H, Briske-Anderson M. Prolonged butyrate treatment inhibits the migration and invasion potential of HT1080 tumor cells. *J Nutr.* 2005; 135:291–295. [PubMed: 15671229]
- Zhang HJ, Zhao W, Venkaraman S, Robbins ME, Buetter GR, Kregel KC, Oberley LW. Activation of matrix metalloproteinase-2 by overexpression of manganese superoxide dismutase in human breast

cancer MCF-7 cells involves reactive oxygen species. *J Biol Chem.* 2002; 277:20919–20926. [PubMed: 11929863]

Zhang Q, Kusaka Y, Sato K, Nakakuki K, Koyama N, Donaldson K. Differences in the extent of inflammation caused by intratracheal exposure to three ultrafine metals: Role of free radical. *J Toxicol Environ Health.* 1998a; 53:423–438.

Zhang Q, Kusaka Y, Sato K, Mo Y, Fukuda M, Donaldson K. Toxicity of ultrafine nickel particle in lung after intratracheal instillation. *J Occup Health.* 1998b; 40:171–176.

Zhang Q, Kusaka Y, Zhu X, Sato K, Mo Y, Kluz T, Donaldson K. Comparative toxicity of standard nickel and ultrafine nickel in lung after intratracheal instillation. *J Occup Health.* 2003; 45:20–32.

Zhao J, Chen H, Davidson T, Kluz T, Zhang Q, Costa M. Nickel-induced 1, 4-alpha-glucan branching enzyme 1 up-regulation via the hypoxic signaling pathway. *Toxicol Appl Pharmacol.* 2004; 196:404–409. [PubMed: 15094311]



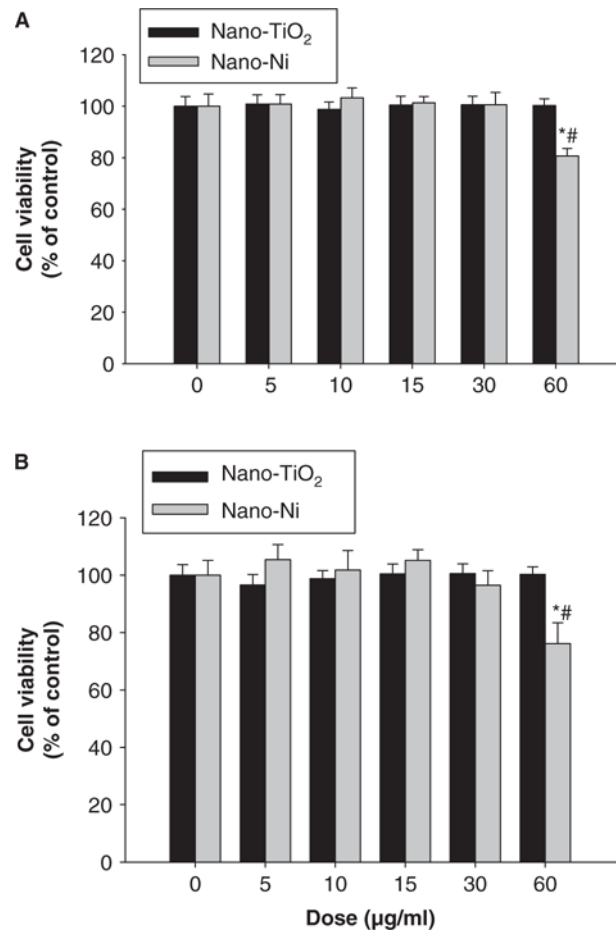


**Figure 1.** Cytotoxic effects of Nano-Ni and Nano-TiO<sub>2</sub> on U937 cells. U937 cells were treated with different doses of Nano-Ni or Nano-TiO<sub>2</sub> for 24 h and cytotoxicity was determined by MTS assay (A) and alamarBlue™ assay (B). U937 cells without treatment were used as control. Values are mean ± SD of six experiments. \*Significant difference from the control,  $p < 0.05$ ; #Significant difference from the same dose of Nano-TiO<sub>2</sub>-treated group,  $p < 0.05$ .

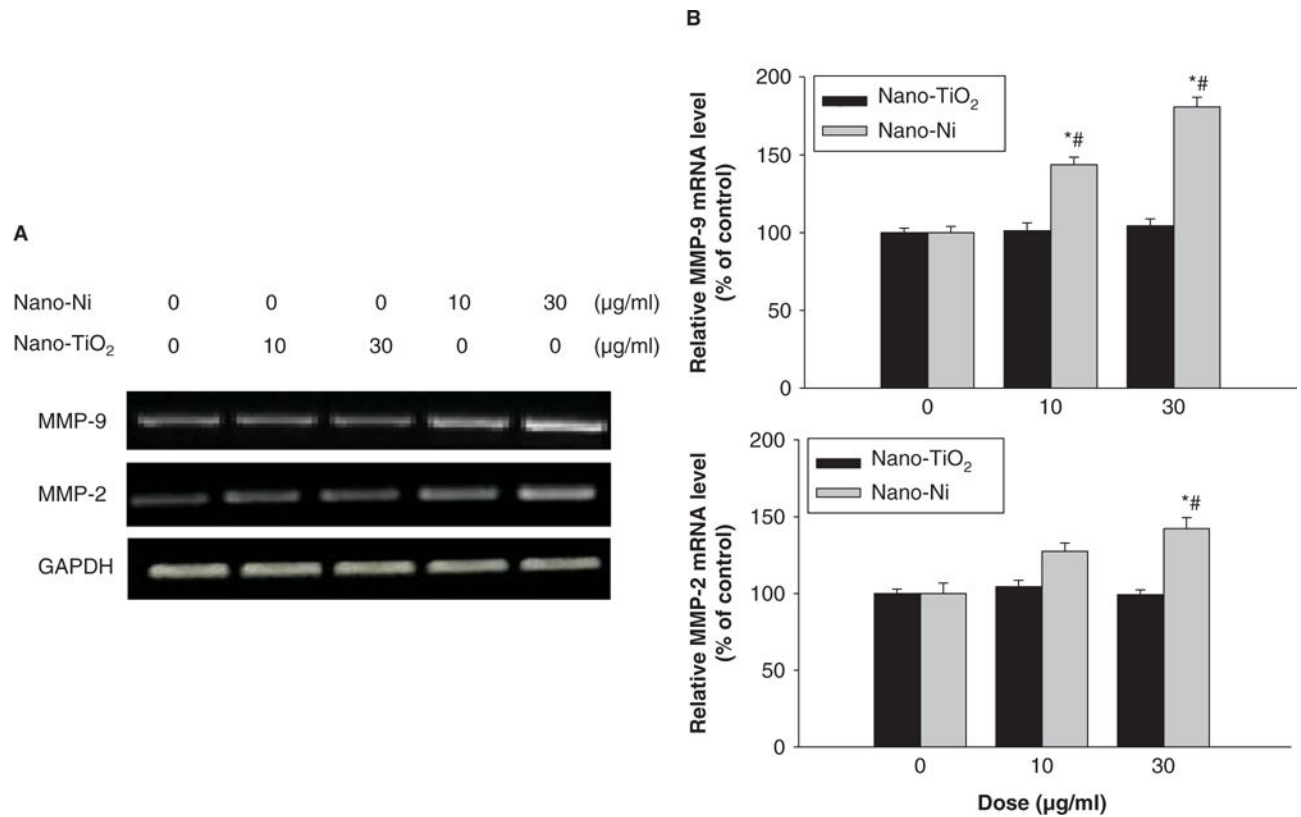


**Figure 2.**

Dose-response induction of MMP-2 and MMP-9 mRNA in U937 cells exposed to Nano-Ni. U937 cells were exposed to 10 or 30  $\mu\text{g/ml}$  of Nano-Ni or Nano-TiO<sub>2</sub> for 24 h. Cells without treatment were used as control. MMP-2 and MMP-9 mRNA expressions were determined by RT-PCR. (A) The results of a single experiment. (B) Normalized band densitometry reading averaged from three independent experiments  $\pm$  SD of RT-PCR results. \*Significant difference as compared with the control,  $p < 0.05$ ; #Significant difference from the same dose of Nano-TiO<sub>2</sub>-treated group,  $p < 0.05$ .

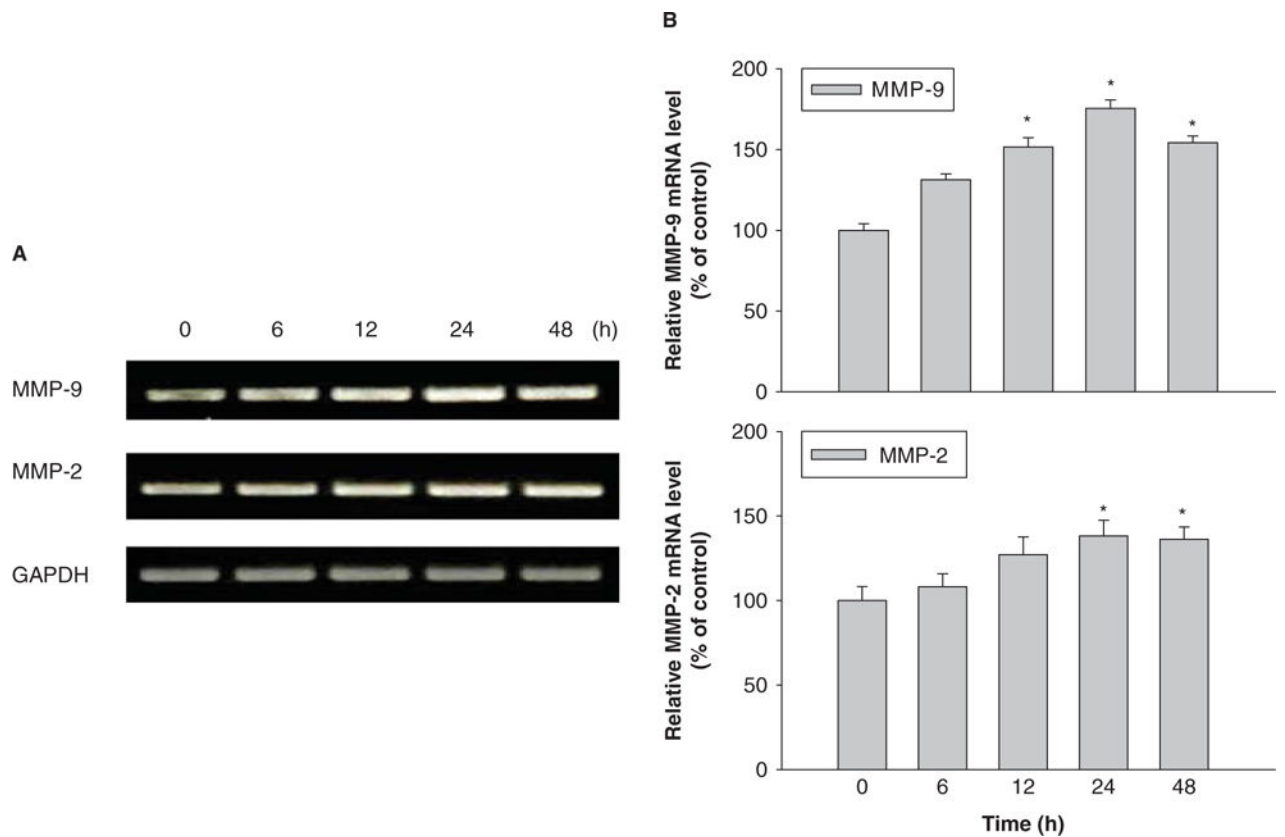


**Figure 3.**

Time-response induction of MMP-2 and MMP-9 mRNA in U937 cells exposed to Nano-Ni. U937 cells were treated with 30  $\mu\text{g/ml}$  of Nano-Ni for 6, 12, 24 and 48 h. Cells without treatment were used as control. MMP-2 and MMP-9 mRNA expression was measured by RT-PCR. (A) The results of a single experiment. (B) Normalized band densitometry readings averaged from three independent experiments  $\pm$  SD of RT-PCR results. \*Significant difference as compared with the control,  $p < 0.05$ .

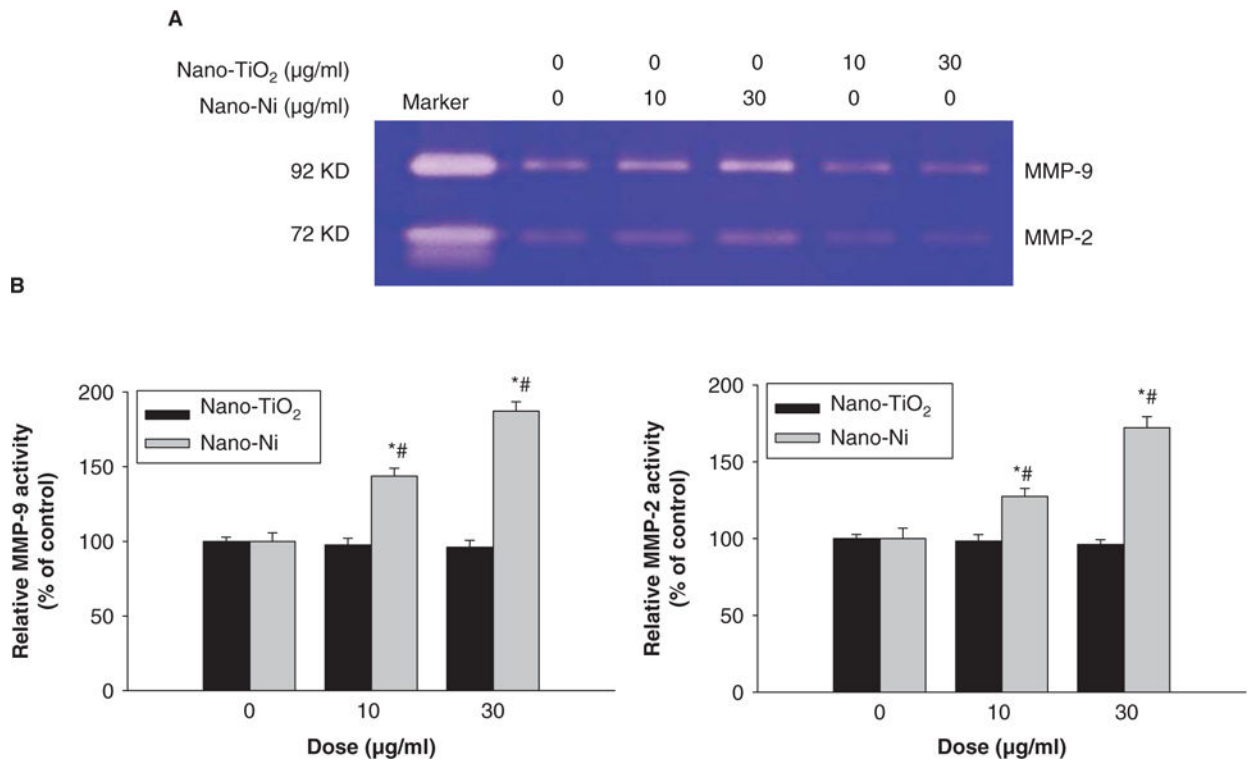


**Figure 4.**

Dose-response increase of pro-MMP-2 and pro-MMP-9 activity in U937 cells exposed to Nano-Ni. Conditioned medium samples were collected after U937 cells were treated with 0, 10 and 30 μg/ml of Nano-TiO<sub>2</sub> or Nano-Ni for 24 h. Cells without treatment were used as control. Pro-MMP-2 and pro-MMP-9 activities were measured by gelatin zymography assay. Supernatants collected from serum-free cultured HT1080 cells were used as a molecular weight marker for pro-MMP-2 and Pro-MMP-9. (A) The results of a single experiment. (B) Normalized band densitometry readings averaged from three independent experiments ± SD of gelatin zymography results. \*Significant difference as compared with the control,  $p < 0.05$ ; #Significant difference as compared with the same dose of Nano-TiO<sub>2</sub>-treated group,  $p < 0.05$ .

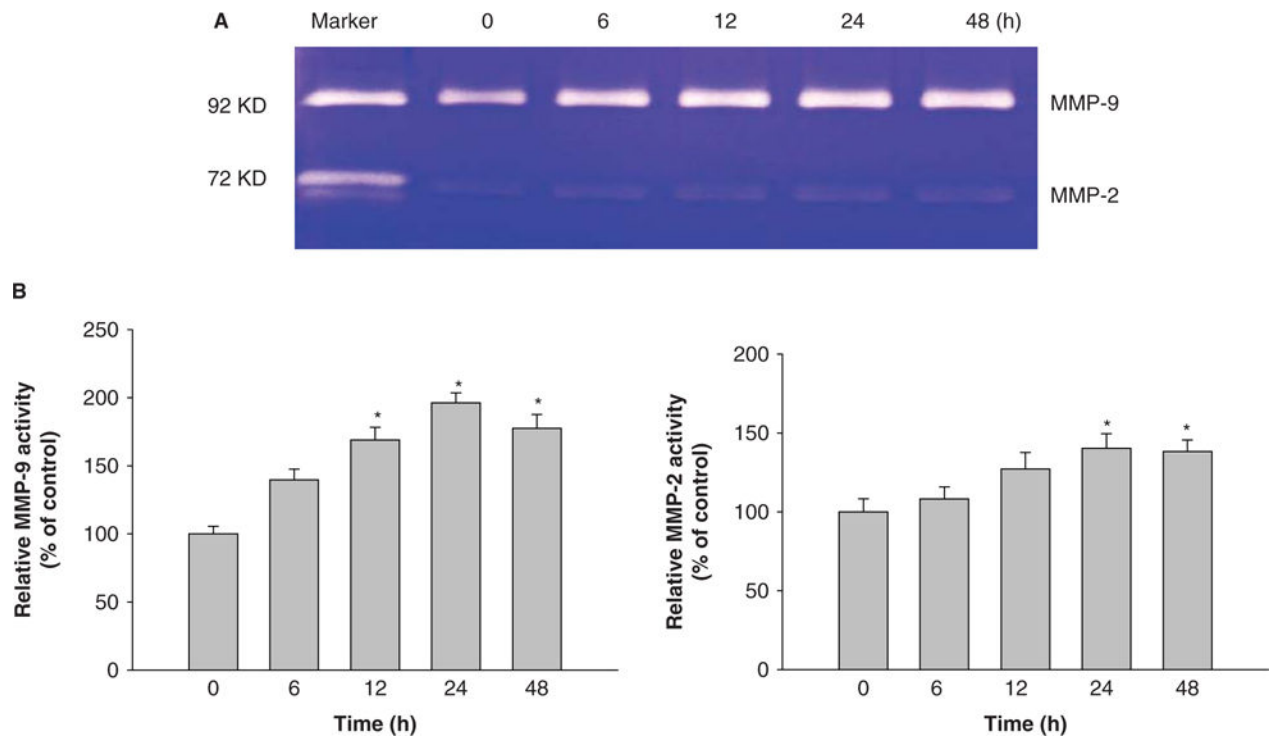


**Figure 5.**

Time-course analysis of pro-MMP-2 and pro-MMP-9 activity in U937 cells exposed to Nano-Ni. Conditioned medium samples were collected after U937 cells were treated with 30  $\mu\text{g}/\text{ml}$  of Nano-Ni for 6, 12, 24 and 48 h. Cells without treatment were used as control. Pro-MMP-2 and pro-MMP-9 activities were measured by gelatin zymography assay.

Supernatants collected from serum-free cultured HT1080 cells were used as a molecular weight marker for pro-MMP-2 and Pro-MMP-9. (A) The results of a single experiment. (B) Normalized band densitometry readings averaged from three independent experiments  $\pm$  SD of gelatin zymography results. \*Significant difference as compared with the control,  $p < 0.05$ .

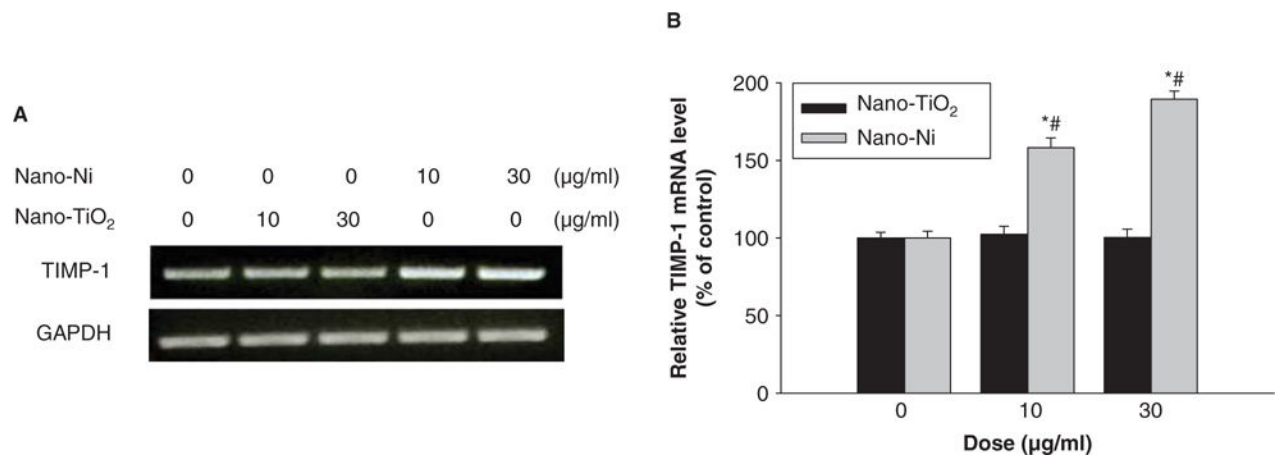


**Figure 6.**

Dose-response induction of TIMP-1 expression in U937 cells exposed to Nano-Ni. U937 cells were exposed to 10 or 30  $\mu\text{g/ml}$  of Nano-Ni or Nano-TiO<sub>2</sub> for 24 h. Cells without treatment were used as control. TIMP-1 mRNA expression was measured by RT-PCR. (A) The results of a single experiment. (B) Normalized band densitometry reading averaged from three independent experiments  $\pm$  SD of RT-PCR results. \*Significant difference as compared with the control,  $p < 0.05$ ; #Significant difference from the same dose of Nano-TiO<sub>2</sub>-treated group,  $p < 0.05$ .



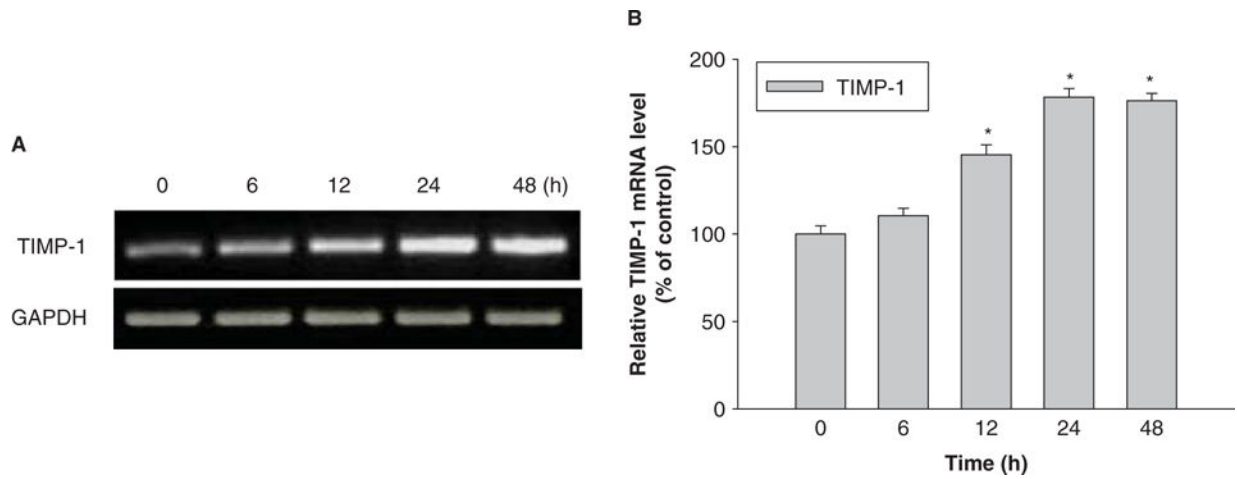


**Figure 7.**

Time-response induction of TIMP-1 in U937 cells exposed to Nano-Ni. U937 cells were treated with 30  $\mu\text{g/ml}$  of Nano-Ni for 6, 12, 24 and 48 h. Cells without treatment were used as controls. TIMP-1 mRNA expression was measured by RT-PCR. (A) The results of a single experiment. (B) Normalized band densitometry readings averaged from three independent experiments  $\pm$  SD of RT-PCR results. \*Significant difference as compared with the control,  $p < 0.05$ .

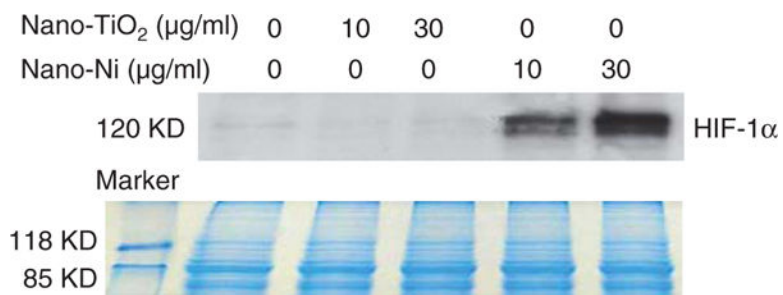


**Figure 8.** Nano-Ni-induced HIF-1 $\alpha$  accumulation in U937 cells. U937 cells were treated with 0, 10 and 30  $\mu\text{g/ml}$  of Nano-TiO<sub>2</sub> or Nano-Ni for 24 h. HIF-1 $\alpha$  nuclear protein was measured by Western blot (upper panel). Equal protein loading was verified by Coomassie Brilliant Blue staining (lower panel).

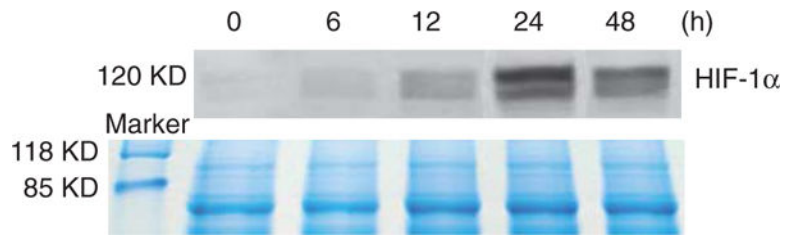


**Figure 9.**

Time-response increase in HIF-1 $\alpha$  expression in U937 cells exposed to Nano-Ni. U937 cells were treated with 30  $\mu$ g/ml of Nano-Ni for 0, 6, 12, 24 and 48 h. HIF-1 $\alpha$  nuclear protein was measured by Western blot (upper panel). Equal protein loading was verified by Coomassie Brilliant Blue staining (lower panel).

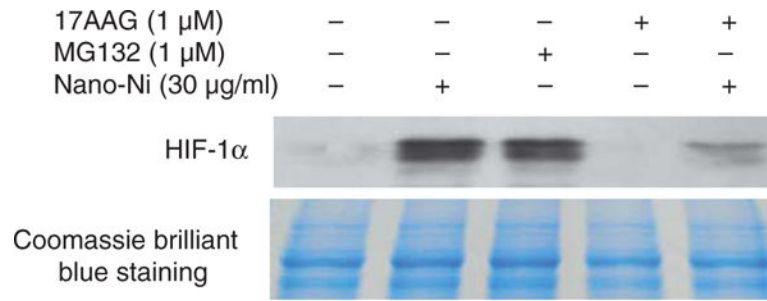


**Figure 10.**

Hsp90 inhibitor, 17-AAG, inhibited Nano-Ni-induced HIF-1 $\alpha$  accumulation in U937 cells. U937 cells were pretreated with 1  $\mu$ M Hsp90 inhibitor, 17-AAG, for 4 h prior to exposure to 30  $\mu$ g/ml of Nano-Ni for another 24 h. Cells treated with proteasome inhibitor MG132 (1  $\mu$ M) were used as positive control for HIF-1 $\alpha$  expression. HIF-1 $\alpha$  nuclear protein was measured by Western blot (upper panel). Equal protein loading was verified by Coomassie Brilliant Blue staining (lower panel).

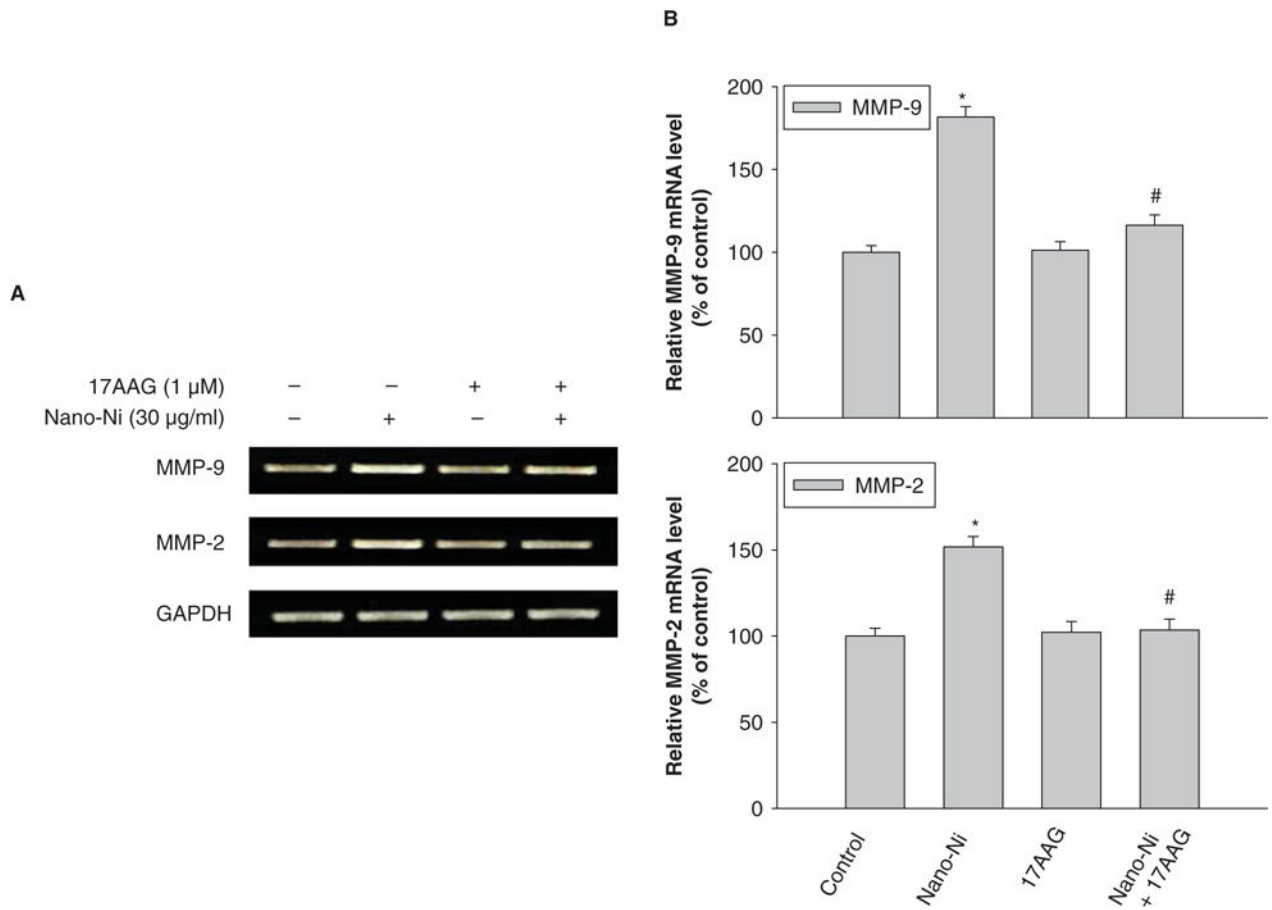


**Figure 11.**

Effects of Hsp90 inhibitor, 17-AAG, on Nano-Ni-induced MMP-2 and MMP-9 upregulation in U937 cells. U937 cells were pretreated with 1  $\mu$ M 17-AAG for 4 h prior to exposure to 30  $\mu$ g/ml of Nano-Ni for another 24 h. Cells without treatment were used as controls. MMP-2 and MMP-9 mRNA expression were measured by RT-PCR. (A) The results of a single experiment. (B) Normalized band densitometry readings averaged from three independent experiments  $\pm$  SD of RT-PCR results. \*Significant difference as compared with the control,  $p < 0.05$ ; #Significant difference as compared with only Nano-Ni-treated group,  $p < 0.05$ .

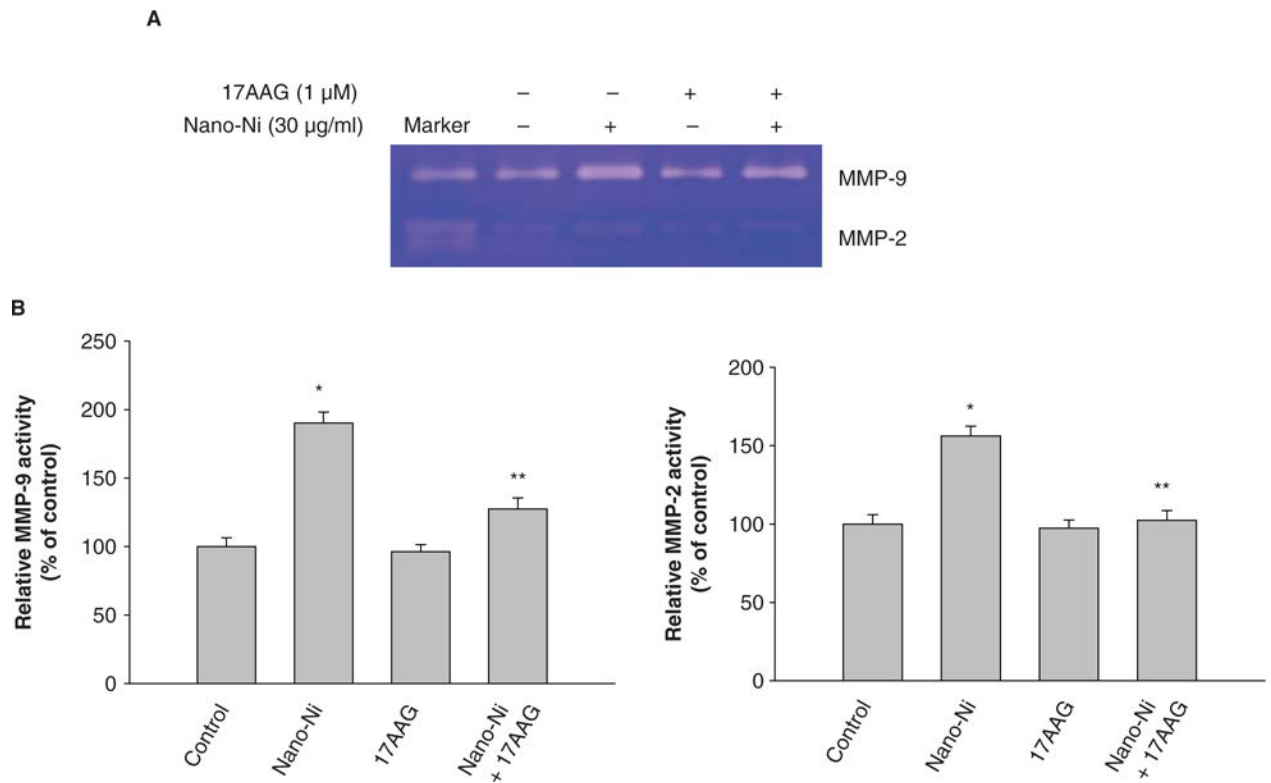


**Figure 12.**

Effects of Hsp90 inhibitor, 17-AAG, on Nano-Ni-induced MMP activities. Conditioned medium samples were collected after U937 cells were pretreated with 17-AAG (1  $\mu$ M) for 4 h prior to exposure to 30  $\mu$ g/ml of Nano-Ni for 24 h. Cells without treatment were used as control. Pro-MMP-2 and pro-MMP-9 activities were measured by gelatin zymography assay. Supernatants collected from serum-free cultured HT1080 cells were used as a molecular weight marker for pro-MMP-2 and Pro-MMP-9. (A) The results of a single experiment. (B) Normalized band densitometry readings averaged from three independent experiments  $\pm$  SD of gelatin zymography results. \*Significant difference as compared with the control,  $p < 0.05$ .



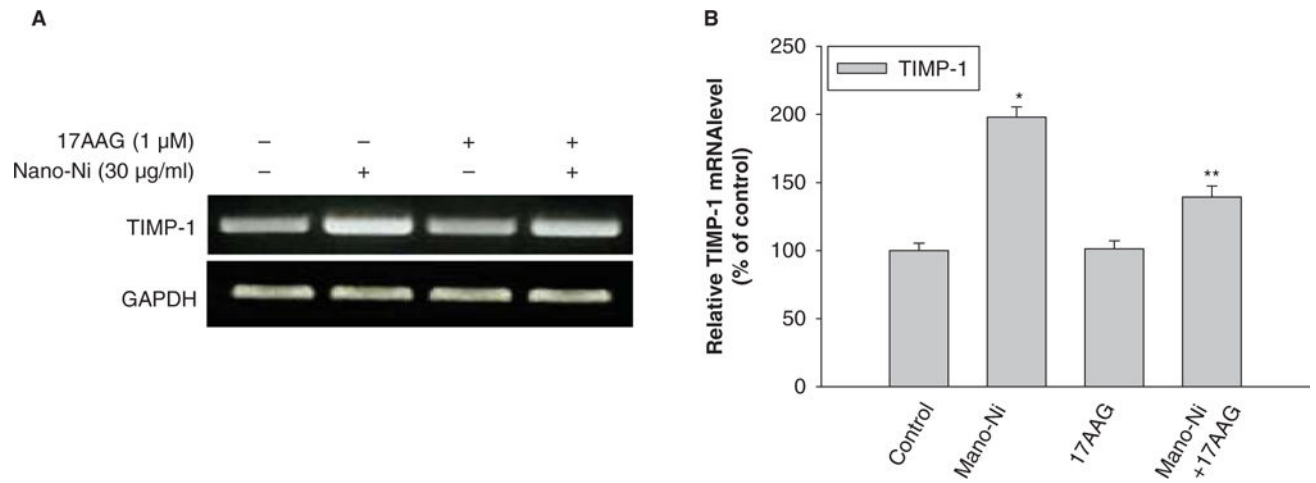


**Figure 13.**

Effects of Hsp90 inhibitor, 17-AAG, on Nano-Ni-induced TIMP-1 mRNA upregulation in U937 cells. U937 cells were pretreated with 1  $\mu$ M 17-AAG for 4 h prior to exposure to 30  $\mu$ g/ml of Nano-Ni for another 24 h. Cells without treatment were used as control. TIMP-1 mRNA expression was measured by RT-PCR. (A) The results of a single experiment. (B) Normalized band densitometry readings averaged from three independent experiments  $\pm$  SD of RT-PCR results. \*Significant difference as compared with the control,  $p < 0.05$ .

**Table I**

Characterization of metal nanoparticles.

Metal	Particle size in powder (Diameter)		DLS (nm) Diameter	TEM (nm) Diameter	Diameter	Specific surface area (m <sup>2</sup> /g)	Phase composition
	(nm, average)	(nm)					
Nano-Ni	20	10–30	250			43.8	Ni (85–90%) NiO (10–15%)
Nano-TiO <sub>2</sub>	28	10–60	280			45.0	Anatase (90%) Rutile (10%)

**Table II**

Solubility of metal nanoparticles in PBS and RPMI-1640.

<b>Metal</b>	<b>PBS (ppm)</b>	<b>RPMI-1640 (ppm)</b>
Nano-Ni	16.48 ± 0.58	81.23 ± 3.74
Nano-TiO <sub>2</sub>	<1.00	<1.00

Author Manuscript

Author Manuscript

Author Manuscript

Author Manuscript